# Figure S1

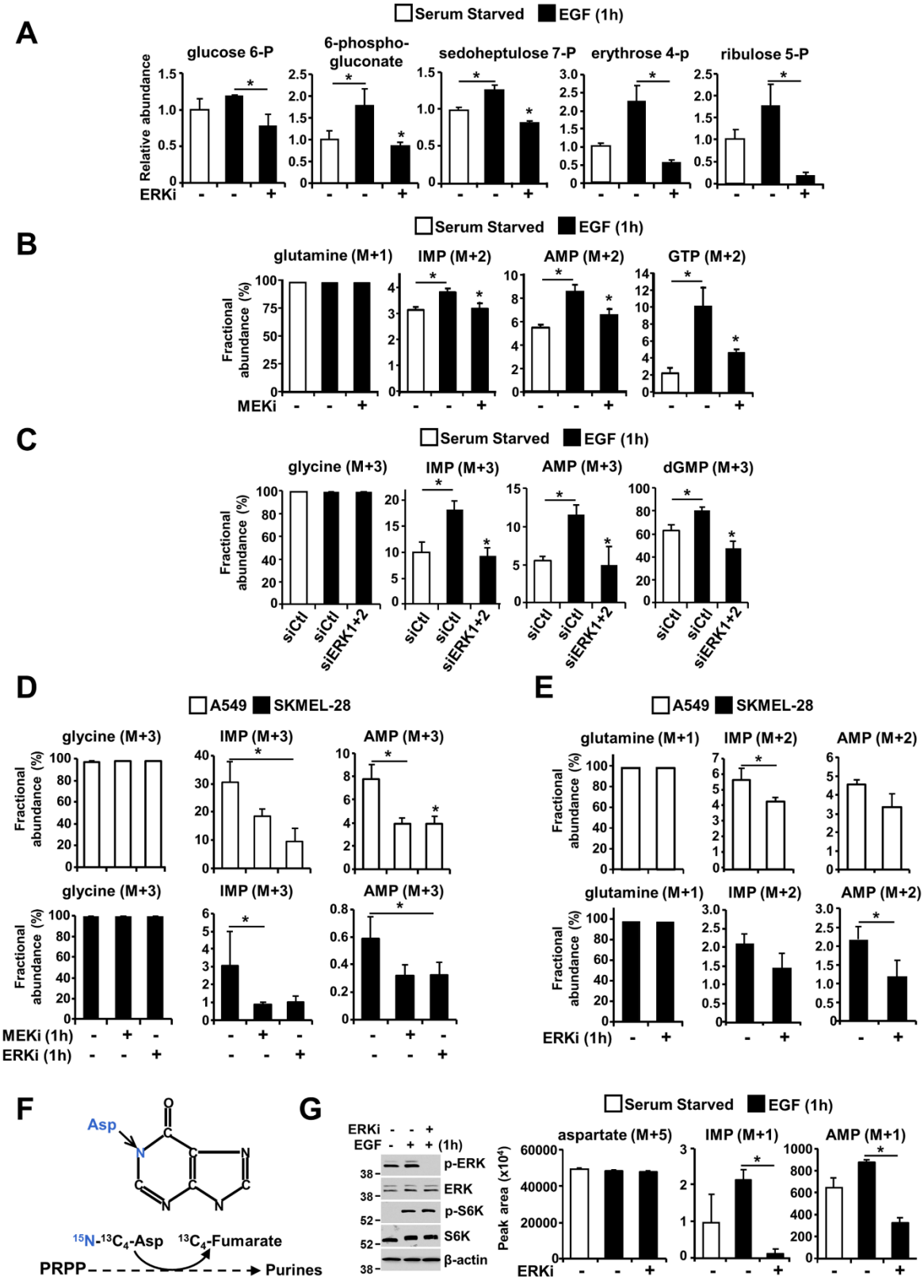
A
Serum Starved
EGF (1h)
glucose 6-P
6-phospho-gluconate
sedoheptulose 7-P
erythrose 4-p
ribulose 5-P
Relative abundance
ERKi
B
glutamine (M+1)
IMP (M+2)
AMP (M+2)
GTP (M+2)
Fractional abundance (%)
MEKi
C
glycine (M+3)
IMP (M+3)
AMP (M+3)
dGMP (M+3)
siCtl
siERK1+2
D
A549
SKMEL-28
MEKi (1h)
ERKi (1h)
E
F
Asp
15N-13C4-Asp
13C4-Fumarate
PRPP
Purines
G
p-ERK
ERK
p-S6K
S6K
β-actin
aspartate (M+5)
IMP (M+1)
AMP (M+1)
Peak area (x10⁴)

**Figure S1. RAS-ERK signaling stimulates de novo purine synthesis. Related to Figure 1.** (A) Relative abundance of metabolites from the pentose phosphate pathway. HeLa cells were serum starved for 15 hours and then pretreated with either vehicle (DMSO) or SCH772984 (ERKi, 1 μM) for 30 min prior to EGF stimulation (50 ng/ml) for 1 hour. Cells were quenched with 80% methanol prior to metabolite extraction. The levels of the pentose phosphate pathway intermediates, as measured via LC-MS/MS, are presented as the means±SDs over three independent samples per condition. (B) The fractional abundances (%) of glutamine (M+1), IMP (M+2), AMP (M+2), and GTP (M+2) from the experimental samples in Figure 1E are shown. C, Fractional abundance (%) of glycine (M+3), IMP (M+3), AMP (M+3), and GMP (M+3) from the experimental samples in Figure 1F are shown. (D) Fractional abundance (%) of glycine (M+3), IMP (M+3), and AMP (M+3) from the experimental samples in Figure 1G are shown. (E) Fractional abundance (%) of glutamine (M+1), IMP (M+2), and AMP (M+2) from A549 and SK-MEL-28 labeled with 15N-(amide)-glutamine for 1 hour treated with either vehicle or SCH772984 (ERKi, 1 hour). (F) Schematic illustrating the incorporation of the nitrogen atom from aspartate into the purine ring. (G) Immunoblots and normalized peak areas of aspartate (M+5), IMP (M+1) and AMP (M+1) as measured by targeted LC-MS/MS from HEK293E cells that were serum starved for 15 hours and pretreated with SCH772984 (ERKi, 1 μM, 30 min) prior to stimulation with EGF (50 ng/ml, 1 hour) labeled with $^{13}C_4$-$^{15}N$-aspartate for the last 30 min. (A-E, G) The data are presented as the means±SDs of three independent samples per condition. * indicates $P<0.05$ for multiple comparisons calculated using a one-way ANOVA with Tukey's honest significant difference (HSD) test or a two-tailed Student's t test for pairwise comparisons

**Figure S2**

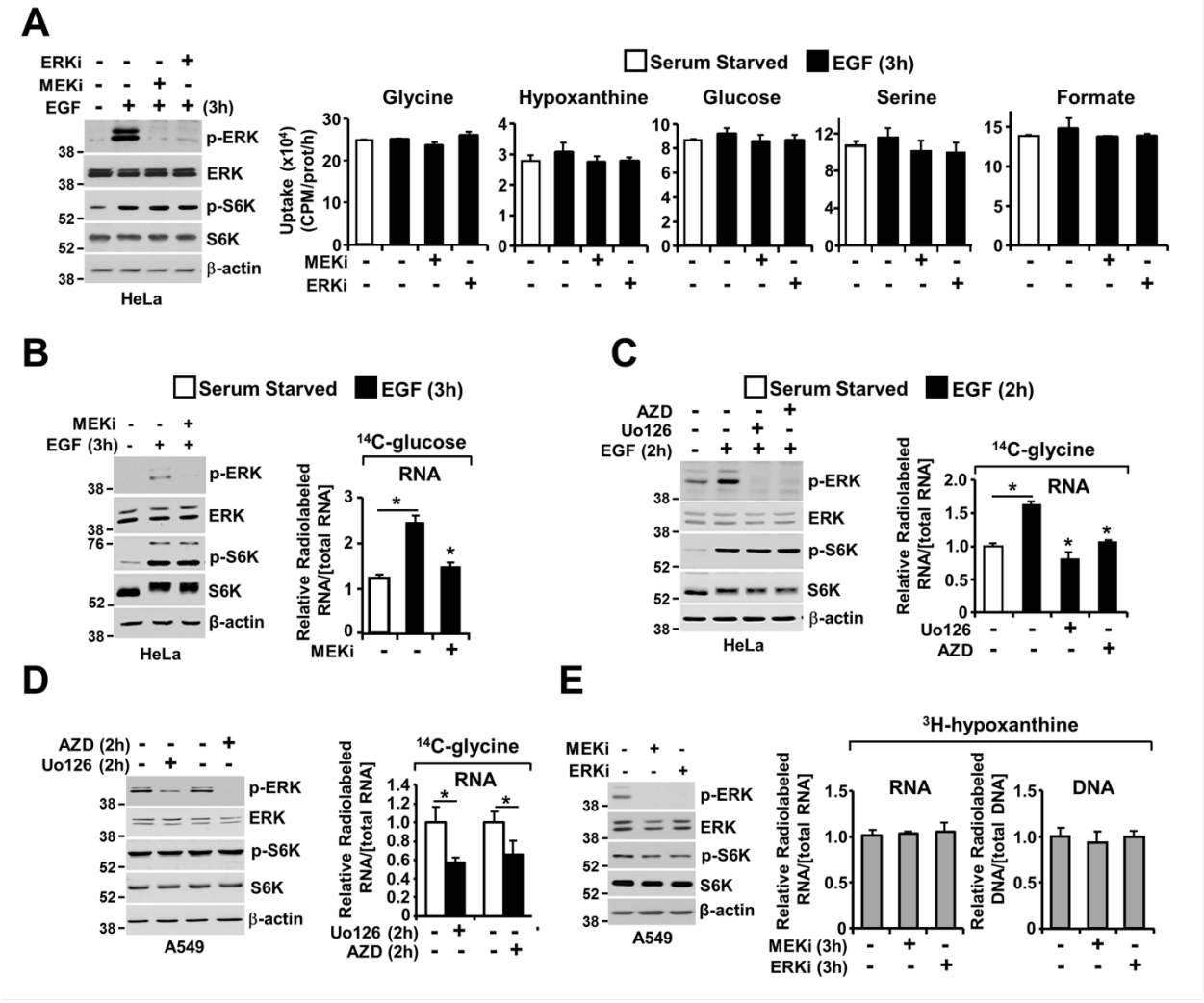


**Figure S2. ERK signaling does not alter the uptake of substrates for de novo purine synthesis. Related to Figure 2**. (A) Representative immunoblots evaluating ERK signaling during the metabolite uptake experiments. The uptake of glycine, hypoxanthine, glucose, serine and formate was not altered by MEK-ERK modulation. HeLa cells were serum starved for 15 hours and treated with vehicle or U0126 (MEKi, 10 μM) or SCH772984 (ERKi, 1 μM) for 30 min prior to EGF (50 ng/ml, 3 hours) stimulation. The uptake of glycine, glucose, serine and formate were measured as the incorporation of $^{14}$C-metabolite over 5 min. Hypoxanthine uptake was measured as the incorporation of $^{3}$H-hypoxanthine over 5 min. The CPM values were normalized to the protein concentration and uptake duration. The data are presented as the means±SDs of two independent experiments. (B) Immunoblot and glucose-derived nucleotide synthesis flux assays with HeLa cells serum starved for 15 hours and stimulated with EGF (50 ng/ml) in the presence or absence of U0126 (MEKi, 10 μM) for 3 hours. Cells were labeled during this 3-hour period with $^{14}$C-glucose, and incorporation of the specific radiolabel into RNA was measured and normalized to the total concentration of RNA. (C) Immunoblot and de novo

purine flux assays with HeLa cells serum starved for 15 hours and stimulated with EGF (50 ng/ml) in the presence or absence of either U0126 (MEKi, 10 μM), or AZD6244 (AZD, 1 μM) for 2 hours. Cells were labeled during this 2-hour period with $^{14}$C-glycine, and incorporation of the specific radiolabel into RNA was measured and normalized to the total concentration of RNA. (D) Immunoblot and de novo purine flux assays with A549 cells serum starved for 15 hours and treated in the presence or absence of either U0126 (MEKi, 10 μM) or AZD6244 (AZD, 1 μM) for 2 hours. Cells were labeled during this 2-hour period with $^{14}$C-glycine, and incorporation of the specific radiolabel into RNA was measured and normalized to the total concentration of RNA. (E) Immunoblot and purine salvage flux assays with A549 cells serum starved for 15 hours and treated in the presence or absence of either U0126 (MEKi, 10 μM) or SCH772984 (ERKi, 1 μM) for 3 hours. Cells were labeled during this 3-hour period with $^{3}$H-hypoxanthine, and incorporation of the specific radiolabel into nucleic acids was measured and normalized to the total concentration of RNA or DNA, as appropriate. The data are presented as the means±SDs of at least two independent experiments. * indicates $P<0.05$ for multiple comparisons calculated using one-way ANOVA with Tukey's HSD test or a two-tailed Student's t test for pairwise comparisons.

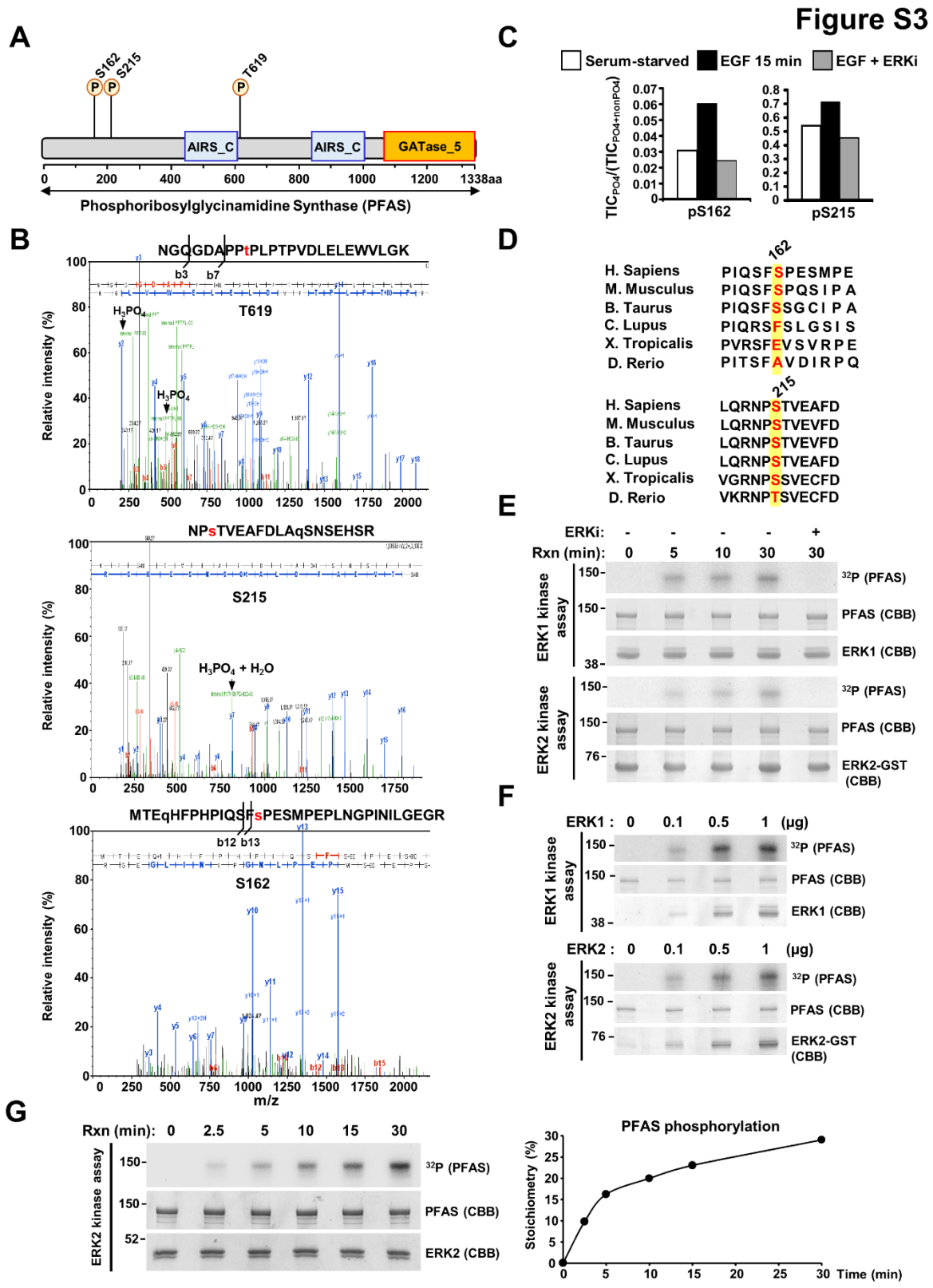


**Figure S3. Stimulation of ERK signaling leads to phosphorylation of PFAS. Related to Figure 4.** (A) Schematic of the primary structure of PFAS depicting the position of the

sites phosphorylated in response to ERK activation. (B) LC-MS/MS spectrum for the triply charged peptide NGQGDAPPtPLPTPVDLELEWVLGK from PFAS indicating a phosphorylation site at T9 in the peptide, corresponding to T619 in the full length PFAS protein. The prominent fragment ions b3 and b7 which include a phosphate group identify the site as corresponding to m/z 554.3. Also shown (below) is the LC-MS/MS spectrum for the doubly charged peptide NPsTVEAFDLAqSNSEHSR from PFAS indicating a phosphorylation site at S3 in the peptide, corresponding to S215 in the full length PFAS protein. The prominent fragment ions b6 and b8 including a phosphate group identify the site as the N-terminal serine residue as well as the doubly charged ion with neutral loss of a phosphate ($H_3PO_4^-$) at m/z 810.5. Finally, the LC-MS/MS tandem mass spectrum for the doubly charged peptide MTEqHFPHPIQSFsPESMPEPLNGPINILGEGR from PFAS indicating a phosphorylation site at S14 of the peptide, corresponding to S162 in the full-length PFAS protein is shown. (C) FLAG-PFAS was immunopurified from serum-starved (15 hours) HEK293E cells treated for 30 min with DMSO or SCH772984 (ERKi, 1 µM) prior to stimulation with EGF (15 min, 50 ng/ml). The ratios of phosphorylated to total peptide levels (S162 and S215), measured as the total ion current (TIC) by LC-MS/MS, of the indicated sites in PFAS under the different conditions are plotted. (D) Sequence conservation of S215 and S162 among PFAS orthologs. (E) Kinase assays with active ERK1 or ERK2 and immunopurified wild-type FLAG-PFAS were performed over the indicated reaction times (Rxn) in the presence or absence of SCH772984 (ERKi, 20 nM) and analyzed by autoradiography. CBB, Coomassie brilliant blue staining. (F) In vitro kinase assays were performed with FLAG-PFAS substrate immunoprecipitated from serum-starved, U0126 (10 µM)-treated HEK-293E cells in the presence of various quantities (µg) of active ERK1 or ERK2 for 15 min and analyzed by autoradiography. (G) As in (E), but the stoichiometry of phosphorylated PFAS was measured over time.

**Figure S4**

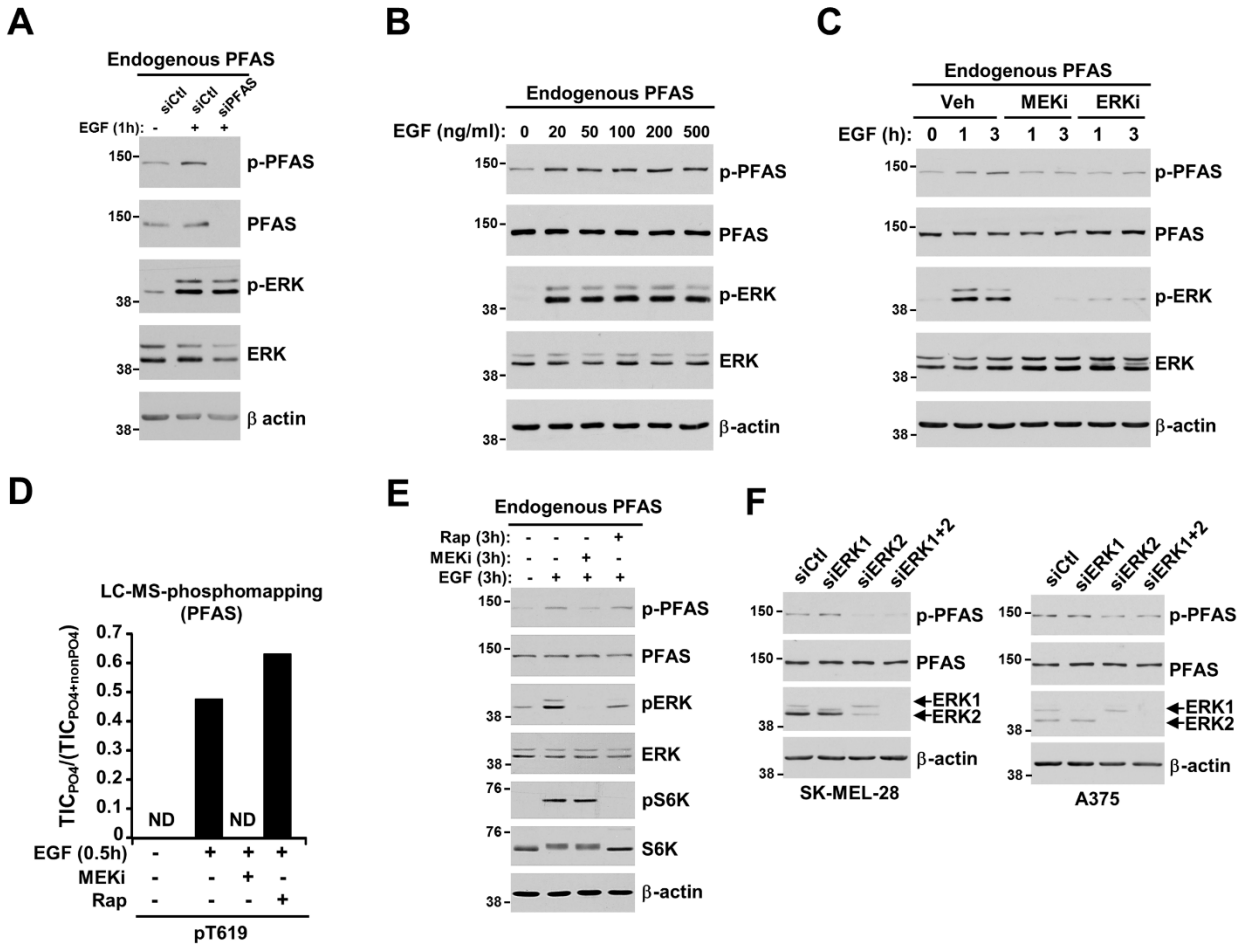


**Figure S4. PFAS is phosphorylated by ERK signaling but not mTORC1. Related to Figure 4.** (A) Immunoblotting validating the recognition of phosphorylated PFAS and PFAS total by the phospho-PFAS antibody in HeLa cells stimulated or not with EGF (1 hour, 50 ng/ml). (B) Immunoblotting assessing phosphorylated PFAS from HeLa cells stimulated with the indicated doses of EGF for 1 hour. (C) HeLa cells were serum-starved (15 hours) and pretreated for 30 min with MEK (U0126, 10 μM) or ERK inhibitor (SCH772984, 1 μM) prior to 1-hour or 3-hour stimulation with EGF (50 ng/mL). (D) Effects of EGF, U0126 (MEKi) and rapamycin (Rap) on the T619 phosphorylation site in PFAS. FLAG-PFAS was immunopurified from serum-starved (15 hours) HEK-293E cells, treated for 30 min with either DMSO or U0126 (10 μM) or rapamycin (20 nM) prior to stimulation with EGF (0.5 hours, 50 ng/ml) and analysed as in (c). ND=phosphopeptide not detected. (E) HeLa cells were serum-starved (15 hours) and pretreated for 30 min with rapamycin (Rap, 20 nM) or MEK inhibitor (U0126, 10 μM) prior to 3-hour stimulation with EGF (50 ng/mL). (F) Immunoblotting from SK-MEL-28 and A375 cells transfected with with siRNAs targeting ERK1, ERK2, or both, or nontargeting controls (siCtl) and stimulated with EGF (50 ng/ml) for the last 3 hours.

Figure S5

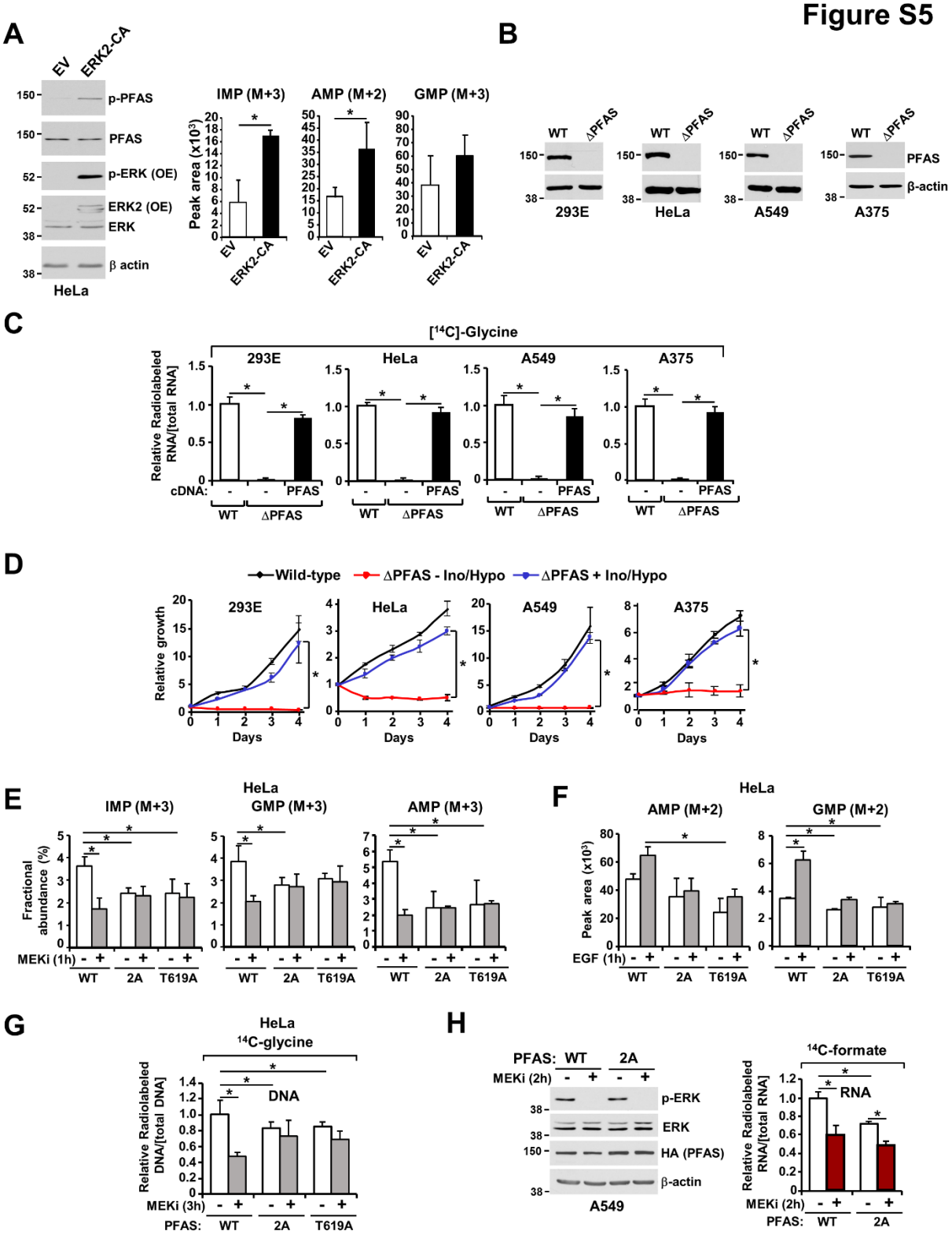


**Figure S5. ERK-mediated PFAS phosphorylation on T619 is required to maintain enhanced purine synthesis in normal and cancer cells. Related to Figure 5.** (A)

Immunoblot and normalized peak areas of $^{15}N$-$^{13}C$-labeled purine intermediates measured in HeLa cells transfected with either empty vector, constitutive active ERK2 (ERK2-CA) and labeled with $^{15}N$-$^{13}C_2$-glycine. (B) Immunoblots validating knockout of PFAS (*ΔPFAS*) in HEK293E, HeLa, A549, and A375 cells. (C) Validation of PFAS loss by assessment of $^{14}C$-glycine flux into nucleic acids. The indicated cell lines—wild-type, *ΔPFAS* or *ΔPFAS* reconstituted with empty-vector or cDNA expressing PFAS were labeled for 4 hours with $^{14}C$-glycine, and incorporation of the specific radiolabel into RNA was measured and normalized to the total concentration of RNA. (D) PFAS knockout cells were auxotrophic for purine nucleosides and nucleobases. The cell proliferation of HEK293E, HeLa, A549, and A375 wild-type or *ΔPFAS* cells cultured in 10% dialyzed serum in the presence or absence of exogenous purines (inosine, 50 µM, and hypoxanthine, 100 µM) was measured over 5 days. (E) The fractional abundances (%) of IMP (M+3), GMP (M+3), and AMP (M+3) from the experimental samples in Figure 5C are shown. (F) Normalized peak areas of AMP (M+2) and GMP (M+2), as measured by targeted LC-MS/MS, from HeLa *ΔPFAS* cells stably reconstituted with wild-type or mutant PFAS (2A or T619A) were serum starved for 15 hours, then stimulated with EGF (50 ng/ml) and concomitant labelling with $^{15}N$-(amide)-glutamine for 1 hour prior to metabolite extraction. (G) HeLa *ΔPFAS* cells expressing wild-type or mutant PFAS (S215A/T619A (2A), T619A) were treated as in Figure 5E and the relative incorporation of $^{14}C$-glycine into DNA was measured and normalized to total concentration of DNA. (H) A549 *ΔPFAS* cells expressing wild-type or mutant PFAS (S215A/T619A (2A)) were serum starved for 15 hours and were then treated with DMSO or U0126 (MEKi, 10 µM) and labeled with $^{14}C$-formate for 2 hours. The relative incorporation of $^{14}C$-formate into RNA was measured and normalized to the total concentration of RNA. The data are presented as the means±SDs of at least two independent experiments (B-H). * indicates $P<0.05$ for pairwise comparison calculated using a two-tailed Student's t test (A) or multiple comparisons calculated using one-way ANOVA with Tukey's HSD test (C-H).

Figure S6

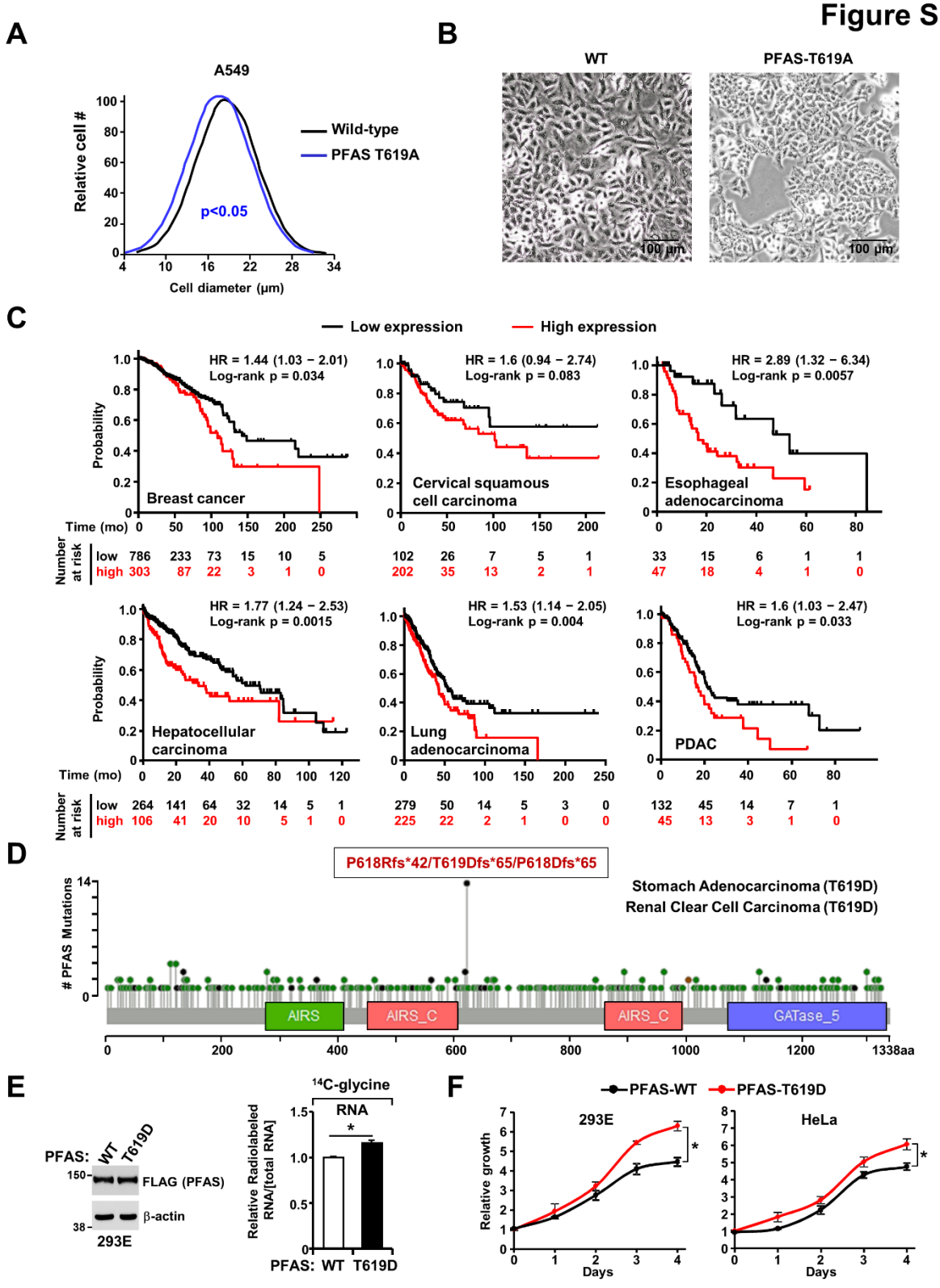


**Figure S6. ERK-mediated PFAS phosphorylation at T619 control cell size and high PFAS expression is associated with poor survival rate in cancer patients. Related**

**to Figure 6.** (A) Effects of ERK-mediated PFAS phosphorylation on cell size. Cell diameter was measured in A549 cells cultured in serum-starved conditions for 24 hours. Color-coded P-values, compared to cells expressing wild-type PFAS, correspond to the color-coding in the legend (>1,000 cells measured for each). (B) A549 cells expressing PFAS variants (wild-type, T619A) under a phase-contrast microscope showing differences in cell size. (C) Survival curves were generated using the Kaplan-Meier Plotter online tool based on data stratified on the best performing threshold for PFAS, KRAS and BRAF mRNA expression. Curves were compared by log-rank test. Survival curves are plotted for all breast cancer patients (n = 1089), cervical squamous cell carcinoma (n = 304), esophageal adenocarcinoma (n = 80), liver hepatocellular carcinoma (n = 370), lung adenocarcinoma (n = 504), and pancreatic ductal adenocarcinoma (n = 177). (D) Summary of all PFAS mutations identified in various cancer types. Identification of a hotspot mutations near the AIRS-C domain of PFAS. Recurrent mutations P618Rfs, T619Dfs, P618Dfs are indicated on the schematic. Data were obtained from The Cancer Genome Atlas (TCGA) c-bioportal (https://www.cbioportal.org/). (E) HEK293E *ΔPFAS* cells stably reconstituted with PFAS-WT or PFAS-T619D were cultured without serum for 15 hours and labeled with $^{14}$C-glycine for 4 hours, and incorporation of the specific radiolabel into RNA was measured and normalized to the total concentration of RNA. (F) The cell proliferation of *ΔPFAS* HEK293E and HeLa cells stably-reconstituted with either wild-type or T619D-PFAS, cultured in 0.5% serum, was measured over 5 days. The data are presented as the means±SDs (E, F). * indicates $P<0.05$ for pairwise comparison calculated using a two-tailed Student's t test (A, E, F).

**Table S1. Selected Reaction Monitoring (SRM) for isotopic tracing experiments. Related to Figure 1, Figure S1, Figure 5, and Figure 6.**

| **SRM for the purine biosynthesis pathway [15N]-glutamine-amide** | | **Q1** | **Collision Energy (CE) (eV)** | **Q3** | |
|---|---|---|---|---|---|
| **Glutamine** | C5H11N2O3+ | 147.1 | 15 | 84.1 | C4H6NO+ |
| **Glutamine_15N** | | 148.1 | | 85.1 | |
| **IMP** | C10H14N4O8P+ | 349 | 19 | 137 | C5H5N4O+ |
| **IMP_15N2** | | 350 | | 139 | |
| **AMP** | C10H15N5O7P+ | 348.15 | 21 | 136 | C5H6N5+ |
| **AMP_15N2** | | 350.15 | | 138 | |
| **GMP** | C10H15N5O8P+ | 364 | 19 | 152 | C5H6N5O+ |
| **GMP_15N2** | | 366 | | 154 | |
| **dAMP** | C10H15N5O6P+ | 332.1 | 21 | 136 | C5H6N5+ |
| **dAMP_15N2** | | 334.1 | | 138 | |
| **GTP** | C10H15N5O14P3- | 522 | -23 | 424 | |
| **GTP_15N2** | | 524 | | 426 | |
| **ADP-nega** | C10H14N5O10P2- | 426.12 | -25 | 159 | HO6P2- |
| **ADP-nega_15N2** | | 428.12 | | 159 | |
| **ATP-nega** | C10H15N5O13P3- | 506.1 | -28 | 159 | HO6P2- |
| **ATP-nega_15N2** | | 508.1 | | 159 | |
| **SRM for the purine biosynthesis pathway [$^{15}$N]-[$^{13}C_2$]-glycine** | | **Q1** | **Collision Energy (CE) (eV)** | **Q3** | |
| **glycine** | $C_2H_6NO_2^+$ | 76.1 | 16 | 30.5 | $CH_4N^+$ |
| **glycine_15N_C2** | | 79.1 | | 32.2 | |
| **IMP** | $C_{10}H_{14}N_4O_8P^+$ | 349 | 19 | 137 | $C_5H_5N_4O^+$ |
| **IMP_15N_13C2** | | 352 | | 140 | |
| **AMP** | $C_{10}H_{15}N_5O_7P^+$ | 348.15 | 21 | 136 | $C_5H_6N_5^+$ |
| **AMP_15N_13C2** | | 351.15 | | 139 | |
| **AMP_13C2** | | 350.15 | | 138 | |
| **GMP** | $C_{10}H_{15}N_5O_8P^+$ | 364 | 19 | 152 | |
| **GMP_15N_13C2** | | 367 | | 155 | |
| **GTP** | $C_{10}H_{15}N_5O_{14}P_3^+$ | 522 | -23 | 424 | |
| **GTP_15N_13C2** | | 525 | | 427 | |

**Table S2. List of q-PCR and mutagenesis primers. Related to Figure 3, Figure 4, Figure 5, Figure 6, and Figure S6.**

| Gene | Species | Primer Forward (5'-->3') | Primer Reverse (5'-->3') | Role/Pathway |
|---|---|---|---|---|
| **RPLP0** | Homo Sapiens | AGCCCAGAACACTGGTCTC | ACTCAGGATTTCAATGGTGCC | Control |
| | | | | |
| **PPAT** | Homo Sapiens | CAGAGGCAATACCATCTCACCTATAA | ACTCGAATGTGTACCTCTTTTGCAC | Purine Synthesis |
| **GART** | Homo Sapiens | AAGGTTATCCTGGAGACTACACCAA | CAGTCCTAGAGCTTGAGCCTCAG | Purine Synthesis |
| **PFAS** | Homo Sapiens | GGATCAAGCCCATCATGTTTAGT | AACCTTTACAACTTCCATGCCTG | Purine Synthesis |
| **PAICS** | Homo Sapiens | GTCTTCTCTTCGACTACCCAGTGG | CAAATTGAGCTGATCCTTCTGGA | Purine Synthesis |
| **ADSL** | Homo Sapiens | GGACCCGCTACAGACAGCAT | CAAACAGATCCGTCGGTTGG | Purine Synthesis |
| **ATIC** | Homo Sapiens | GAACCATTGGCGAGGATGAA | GCCTCAGTGAGTAACTCAGGGACT | Purine Synthesis |
| **ADSS** | Homo Sapiens | CAAAGTTGGAGTTGCTTACAAGTTAG | CCTGGGAGAGTCTTATATTGAACTTC | Purine Synthesis |
| **IMPDH1** | Homo Sapiens | CCGCAGCCTGTCTGTCCT | CCGACATGGTCCGCTTCT | Purine Synthesis |
| **IMPDH2** | Homo Sapiens | AGTGGCTCCATCTGCATTACG | ACCTTGTACACTGCTGTTGCTTG | Purine Synthesis |
| **GMPS** | Homo Sapiens | CCAATTAAAACTGTAGGTGTGCAGG | TCTTTACTGGAGATTCCACACACG | Purine Synthesis |
| **Mutagenesis primers** | | | | |
| **PFAS_ S162A** | Homo Sapiens | CATGCTCTCAGGGGCGAAACTCTG GATGGG | CCCATCCAGAGTTTCGCCCCTGAGA GCATGC | PFAS mutation |
| **PFAS_ S215A** | Homo Sapiens | GGCCTCCACAGTGGCCGGGTTCCG CTGT | ACAGCGGAACCCGGCCACTGTGGA GGCC | PFAS mutation |
| **PFAS_ T619A** | Homo Sapiens | TGGCAGGGGTGCCGGGGGGGCAT | ATGCCCCCCCGGCACCCCTGCCA | PFAS mutation |
| **PFAS_ T619D** | Homo Sapiens | GGGGTTGGCAGGGGATCCGGGGG GGCATCCC | GGGATGCCCCCCCGGATCCCCTG CCAACCCC | PFAS mutation |
| **ERK2_ L73P** | Homo Sapiens | CTGAGAGAGATAAAAATCCCACTGCG CTTCAGACATG | CATGTCTGAAGCGCAGTGGGATT TTTATCTCTCTCAG | ERK2 mutation |
| **ERK2_ S151D** | Homo Sapiens | CCGTGACCTCAAGCCTGACAACCTCC TGCTGAAC | GTTCAGCAGGAGGTTGTCAGGCT TGAGGTCACGG | ERK2 mutation |